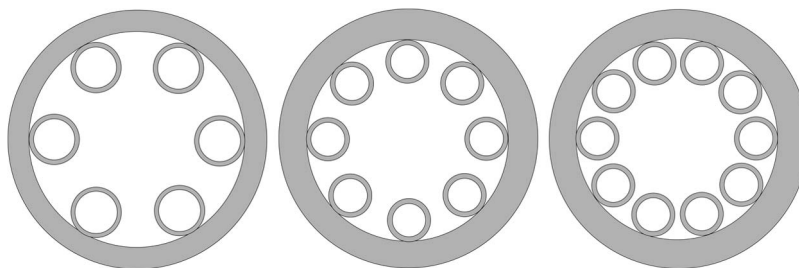


Impact of Cladding Tubes in Chalcogenide Negative Curvature Fibers

Volume 8, Number 3, June 2016

Chengli Wei
Curtis R. Menyuk
Jonathan Hu



DOI: 10.1109/JPHOT.2016.2577711
1943-0655 © 2016 IEEE

Impact of Cladding Tubes in Chalcogenide Negative Curvature Fibers

Chengli Wei,¹ Curtis R. Menyuk,² and Jonathan Hu¹

¹Department of Electrical and Computer Engineering, Baylor University, Waco, TX 76798 USA

²Department of Computer Science and Electrical Engineering, University of Maryland
Baltimore County, Baltimore, MD 21227 USA

DOI: 10.1109/JPHOT.2016.2577711

1943-0655 © 2016 IEEE. Translations and content mining are permitted for academic research only.

Personal use is also permitted, but republication/redistribution requires IEEE permission.

See http://www.ieee.org/publications_standards/publications/rights/index.html for more information.

Manuscript received February 11, 2016; revised June 1, 2016; accepted June 3, 2016. Date of publication June 7, 2016; date of current version June 17, 2016. This work was supported in part by funds from the Vice Provost for Research at Baylor University. The work of C. R. Menyuk was supported by the Naval Research Laboratory. Corresponding author: J. Hu (e-mail: jonathan_hu@baylor.edu).

Abstract: We computationally study the leakage loss and bandwidth in chalcogenide negative curvature fibers. The leakage loss is decreased by a factor of 19, and the operating bandwidth is almost doubled when the optimal gap between cladding tubes is used in negative curvature fibers with six tubes. There is a wide range of the gaps between 5 and 40 μm , which gives a leakage loss lower than 0.04 dB/m and a wide transmission bandwidth of 1.1 μm . The optimal gap in a fiber with six cladding tubes is three times as large as the optimal gap in fibers with eight or ten cladding tubes. A larger gap is needed in a fiber with six cladding tubes to remove the weak coupling between the central core mode and the tube modes. This design of the chalcogenide negative curvature fibers using a wide range of gaps will lead to successful fiber devices with a low loss and a wide bandwidth for mid-IR transmission.

Index Terms: Waveguides, MWIR devices, fiber optics systems, modeling.

1. Introduction

Hollow-core photonic bandgap fibers using a periodic cladding structure with an air core in the center have attracted great interest due to their promise to realize a unique range of optical properties that are not possible in conventional fibers [1]–[5]. Recently, a new kind of air core fiber, negative curvature fibers consisting of a ring of tubes, have yielded promising results with low transmission loss [6]–[18]. Negative curvature means that the surface normal to the core boundary is oppositely directed from the core [19]–[21]. Antiresonant reflection is the guiding mechanism in the negative curvature fibers [22], [23]. Since no bandgap is used, there is no requirement for a periodic cladding structure. The development of hollow-core chalcogenide fibers has been hampered by fabrication difficulties. This simple negative curvature structure could be used to fabricate fiber devices using non-silica glasses, such as chalcogenides. The delivery of mid-infrared radiation has been successfully demonstrated using chalcogenide negative curvature fibers [21], [24], [25].

It is found that a gap between cladding tubes can effectively decrease the leakage loss in negative curvature fibers [26]–[28]. When the tubes touch, localized nodes are created, and modes exist in the localized node area. A separation between the cladding tubes removes the additional resonances in the transmission bands [26], [27]. However, further increase in the

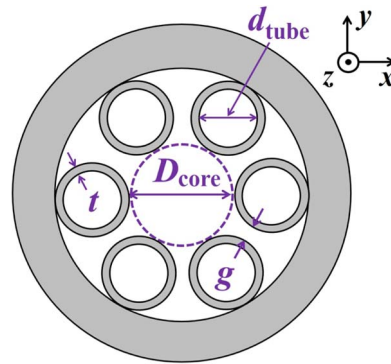


Fig. 1. Cross section of the chalcogenide negative curvature fiber with six cladding tubes.

separation between the cladding tubes decreases the mode confinement in the air core. There is an optimal gap range between these two limits. In addition, the surface tension forces straighten the tube walls in the fiber drawing process [26]. Hence, it is difficult to obtain touching circular tubes to produce a negative curvature core boundary. In a negative curvature fiber whose cladding tubes do not touch, it is possible to maintain the circular shape of the tubes even at a high drawing temperature [26]. Hence, fibers with a gap between tubes are expected easier to fabricate, since surface tension would naturally assist in maintaining the circular shape of the tubes.

Sources and transmission of mid-infrared light are important for applications in biosensing, environmental monitoring, homeland security, and medical diagnostics [29]. In this paper, we computationally study the leakage loss [30] and bandwidth in chalcogenide negative curvature fibers with 6 cladding tubes at a wavelength of $5 \mu\text{m}$. We focus on $5 \mu\text{m}$ because development of quantum cascade lasers has shown great potential for the generation of mid-infrared emission around $5 \mu\text{m}$ with a wall-plug efficiency of 50% and a watt-level power output [31]. We show that the leakage loss decreases and bandwidth increases with an appropriate gap between cladding tubes. Using a fiber with a tube wall thickness of $1.8 \mu\text{m}$ and a gap range between $5 \mu\text{m}$ and $40 \mu\text{m}$, a low transmission loss of under 0.04 dB/m and a bandwidth of $1.1 \mu\text{m}$ can be achieved simultaneously for chalcogenide negative curvature fibers with 6 cladding tubes. We also compare the optimal gaps for fibers with 6, 8, and 10 cladding tubes. We find that the optimal gap in a fiber with 6 cladding tubes is 3 times as large as the optimal gap in fibers with 8 or 10 cladding tubes. The reason is that there is a weak coupling between the central core mode and the tube modes in a fiber with 6 cladding tubes. A larger gap is needed to remove the weak coupling.

2. Geometry

In this section, we show the geometry of the negative curvature fibers. Fig. 1 shows the full hollow-core fiber geometry with 6 tubes in the cladding. Only a quarter of the geometry is used in modeling hollow-core negative curvature fibers because of the symmetry of the modes [32]–[34]. The gray regions represent glass, and the white regions represent air. The inner tube diameter, d_{tube} , the core diameter, D_{core} , the tube wall thickness, t , the number of tubes, k , and the minimum gap between the cladding tubes, g , have the following relationship: $D_{\text{core}} = (d_{\text{tube}} + 2t + g)/\sin(\pi/k) - (d_{\text{tube}} + 2t)$ [14], [35]. The core diameter, D_{core} , is fixed at $150 \mu\text{m}$, and the ratio of the core diameter to the wavelength is $D_{\text{core}}/\lambda = 30$. Different negative curvature fibers were fabricated using a ratio of the core diameter to the wavelength that varies from 31 to 36 [6], [7], [27], [28]. We calculate the fiber modes and their propagation constants using Comsol Multiphysics, a commercial full-vector mode solver that uses the finite-element method. Anisotropic, perfectly matched layers (PMLs) are positioned outside the cladding in

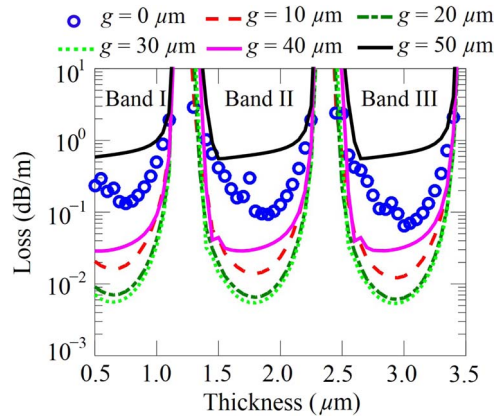


Fig. 2. Leakage loss as a function of tube wall thickness with different gaps. The wavelength is $5 \mu\text{m}$.

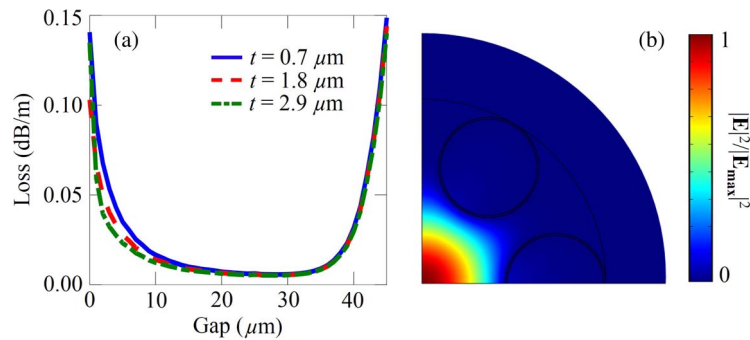


Fig. 3. (a) Leakage loss as a function of the gap with different tube wall thicknesses of 0.7, 1.8, and $2.9 \mu\text{m}$ and with a wavelength of $5 \mu\text{m}$. (b) Normalized mode intensity in the fiber with a gap of $30 \mu\text{m}$ and a tube thickness of $1.8 \mu\text{m}$.

order to reduce the size of the simulation window [36]. We simulate As_2S_3 chalcogenide glass with a refractive index whose real part equals 2.4 and whose imaginary part equals 3.4×10^{-8} at a wavelength $\lambda = 5 \mu\text{m}$ [37].

3. Leakage Loss

In this section, we study the leakage loss in chalcogenide fibers with different tube wall thicknesses and different gaps between the cladding tubes. Fig. 2 shows the leakage loss as a function of tube wall thickness for a fiber with different gaps when the tube wall thickness increases from $0.5 \mu\text{m}$ to $3.5 \mu\text{m}$. There are three thicknesses at $t = 1.2 \mu\text{m}$, $2.4 \mu\text{m}$, and $3.5 \mu\text{m}$, near which high loss occurs. These tube wall thicknesses match the resonance condition, $t = m\lambda/[2(n_1^2 - n_0^2)^{1/2}]$, where m equals any positive integer, λ is the light wavelength, and $n_1 = 2.4$ and $n_0 = 1.0$ are the refractive indices of chalcogenide glass and air, respectively [22], [23]. We show the first three transmission bands, labeled I, II, and III, that occur between the three tube wall thicknesses, at which high loss is present. The tube wall thicknesses corresponding to the minimum loss for these three transmission bands are located at $0.7 \mu\text{m}$, $1.8 \mu\text{m}$, and $2.9 \mu\text{m}$. These values are consistent with the antiresonance condition, $t = (m - 0.5)\lambda/[2(n_1^2 - n_0^2)^{1/2}]$, where m equals any positive integer [22], [23]. The tube wall thickness corresponding to the minimum loss only changes slightly when the gap increases from $10 \mu\text{m}$ to $40 \mu\text{m}$.

In Fig. 3(a), we plot the leakage loss as a function of the gap with tube wall thicknesses of $0.7 \mu\text{m}$, $1.8 \mu\text{m}$, and $2.9 \mu\text{m}$. The leakage loss decreases when the gap is first introduced, and

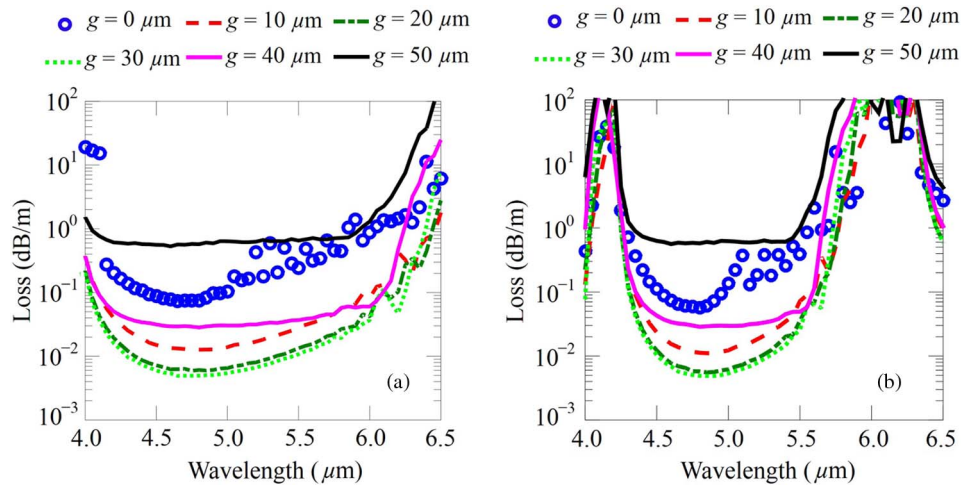


Fig. 4. Leakage loss as a function of wavelength with different gaps for tube thicknesses of (a) $1.8 \mu\text{m}$ and (b) $2.9 \mu\text{m}$.

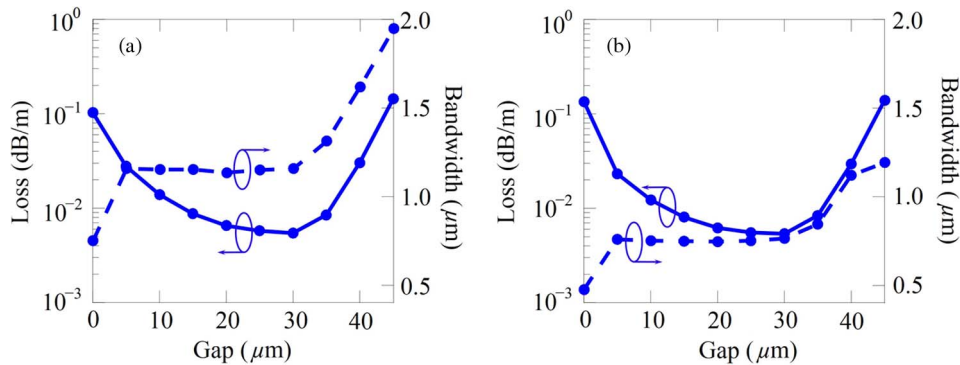


Fig. 5. Loss at a wavelength of $5 \mu\text{m}$ and bandwidth as a function of the gap for tube wall thicknesses of (a) $1.8 \mu\text{m}$ and (b) $2.9 \mu\text{m}$.

the leakage loss increases as the gap increases. When there is no gap, two nearby tubes create nodes where the mode field can reside [26], [27]. However, when the gap is too large, the field leaks through the gap, and the leakage loss increases. Fig. 3(b) shows the normalized mode intensity in the fiber with a gap of $30 \mu\text{m}$, a tube thickness of $1.8 \mu\text{m}$, and a wavelength of $5 \mu\text{m}$.

We also studied the leakage loss as a function of wavelength with different gaps. Fig. 4(a) and (b) shows the results with tube wall thicknesses of $1.8 \mu\text{m}$ and $2.9 \mu\text{m}$, respectively, corresponding to the tube wall thicknesses of transmission bands II and III in Fig. 2. The material dispersion is also included in the simulation [38], [39]. Again, the leakage loss can be decreased when an appropriate gap is used. The minimum loss occurs at a wavelength slightly lower than $5 \mu\text{m}$ because the core size is effectively larger at a smaller wavelength. The differences between the losses at a wavelength of $5 \mu\text{m}$ and at the wavelengths corresponding to the minimum loss, which is near $4.8 \mu\text{m}$, is only 11% and 12% for thicknesses of $1.8 \mu\text{m}$ and $2.9 \mu\text{m}$, respectively, between gaps of $10 \mu\text{m}$ and $40 \mu\text{m}$. We also confirmed that the minimum loss occurs at a wavelength slightly lower than $5 \mu\text{m}$ even when the material dispersion is neglected.

We also plot the leakage loss at $5 \mu\text{m}$ as a function of the gap for thicknesses of $1.8 \mu\text{m}$ and $2.9 \mu\text{m}$ using the blue solid curves in Fig. 5(a) and (b), respectively. The leakage loss can be

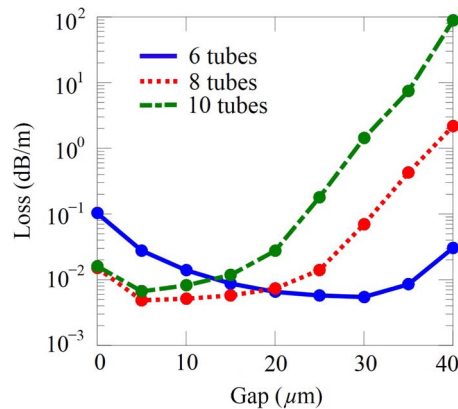


Fig. 6. Leakage loss as a function of gap in fibers with six, eight, and 10 cladding tubes. The tube wall thickness is $1.8 \mu\text{m}$, and the wavelength is $5 \mu\text{m}$.

decreased by factors of 19 and 25 for thicknesses of $1.8 \mu\text{m}$ and $2.9 \mu\text{m}$, respectively, when an appropriate gap is used.

4. Bandwidth

Bandwidth is another important parameter. Here, we define the bandwidth as the transmission window where the leakage loss is less than twice the minimum leakage loss. The bandwidth as a function of the gap for both thicknesses of $1.8 \mu\text{m}$ and $2.9 \mu\text{m}$ is shown using the blue dashed curves in Fig. 5(a) and (b), respectively. When the gap increases from $g = 0$ to $g = 5 \mu\text{m}$, the bandwidth increases sharply. When the gap increases from $g = 5 \mu\text{m}$ to $g = 30 \mu\text{m}$, the bandwidth stays almost the same. When the gap increases from $g = 30 \mu\text{m}$ to $g = 42.5 \mu\text{m}$, the bandwidth further increases with the tradeoff that the minimum loss at the center of the transmission band increases, as shown in Fig. 5. The bandwidth for a tube wall thickness of $1.8 \mu\text{m}$ in Band II is wider than the bandwidth for a tube wall thickness of $2.9 \mu\text{m}$ in Band III, as shown in both Figs. 4 and 5. In negative curvature fibers, the operating wavelength sits between the nearby resonance wavelengths at $\lambda = 2t(n_1^2 - n_0^2)^{1/2}/m$, where m equals any positive integer and t is the tube wall thickness. Hence, a lower-order transmission band with a smaller m will yield a wider bandwidth.

Comparing the leakage loss and bandwidth in Fig. 5, the gap should be chosen in the range between $5 \mu\text{m}$ and $40 \mu\text{m}$, depending on the tradeoff between loss and bandwidth in specific applications. When the gap is between $5 \mu\text{m}$ and $40 \mu\text{m}$, the bandwidth can be $1.1 \mu\text{m}$ and $0.75 \mu\text{m}$ in the fibers with tube wall thicknesses of $1.8 \mu\text{m}$ and $2.9 \mu\text{m}$, respectively. The corresponding ratios of the bandwidth to the central wavelength are 22% and 15%. Meanwhile, the losses at $5 \mu\text{m}$ can be lower than 0.04 dB/m in both fibers. The broad range of gaps that have nearly minimum loss allows successful fiber devices as it might be hard to exactly control the size of the gap in the fiber drawing process.

5. Number of Tubes

In previous sections, we studied the leakage loss and the bandwidth in negative curvature fibers with 6 cladding tubes. In this section, we study the effect of the gap on the leakage loss and the bandwidth in fibers with 8 and 10 cladding tubes. The core diameter, the tube wall thickness, and the wavelength are fixed at $150 \mu\text{m}$, $1.8 \mu\text{m}$, and $5 \mu\text{m}$, respectively. We only study the transmission Band II at a tube wall thickness of $1.8 \mu\text{m}$ in this section, because we find no significant difference in leakage loss between Band II and Band III, as shown in Figs. 3–5. Fig. 6 shows the leakage loss as a function of the gap for fibers with 6, 8, and 10 cladding tubes. The blue solid curve shows the leakage loss of a fiber with 6 cladding tubes, which is the same as the blue solid curve in Fig. 5(a). For a fiber with 6 cladding tubes, the leakage loss decreases

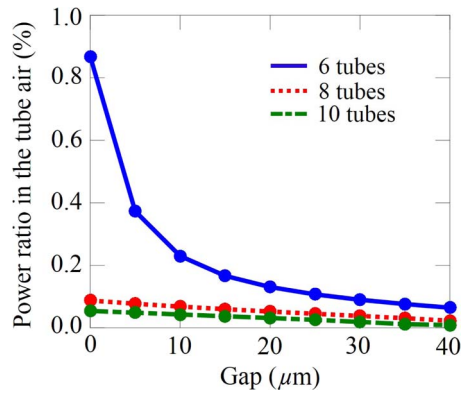


Fig. 7. Power ratio inside the tubes as a function of the gap in fibers with six, eight, and ten cladding tubes. The tube wall thickness is $1.8 \mu\text{m}$, and the wavelength is $5 \mu\text{m}$.

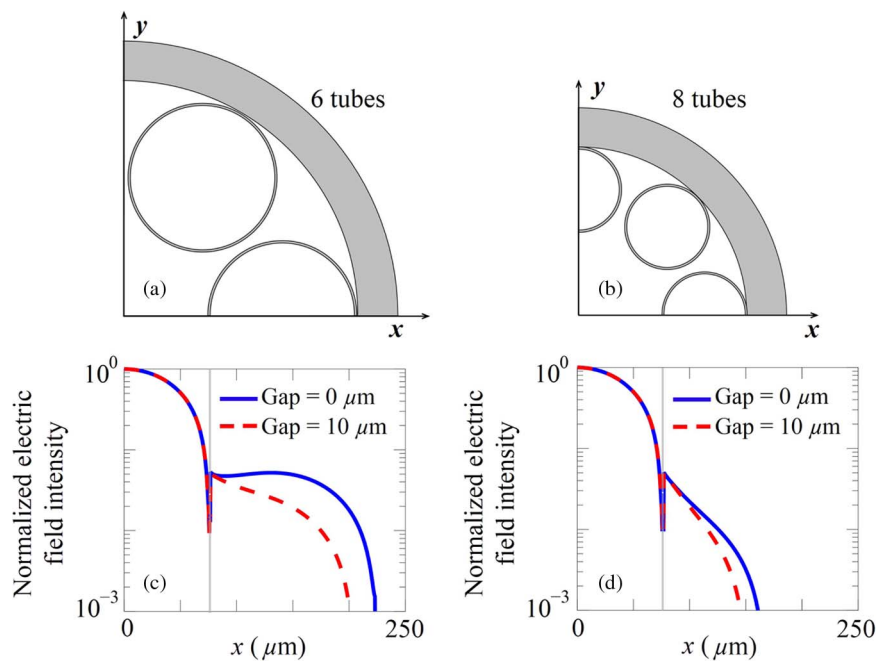


Fig. 8. Normalized electric field intensity at $g = 0$ and $g = 10 \mu\text{m}$ in fibers with (a) six and (b) eight cladding tubes. The tube wall thickness is $1.8 \mu\text{m}$, and the wavelength is $5 \mu\text{m}$. The thin gray vertical bars indicate the location of the glass tube at $x = 75 \mu\text{m}$ with a thickness of $1.8 \mu\text{m}$.

by a factor of 19 when an appropriate gap is used. For fibers with 8 and 10 cladding tubes, the leakage losses only decrease by 66% and 49% when the gap increases from 0 to $10 \mu\text{m}$, respectively. The optimal gap in a fiber with 6 cladding tubes is 3 times as large as the optimal gap in fibers with 8 or 10 cladding tubes.

In order to find the reason for the difference between the behavior with 6, 8, and 10 cladding tubes, we plot the power ratio inside the tubes for fibers with 6, 8, and 10 cladding tubes in Fig. 7. The power ratio inside the tubes is defined as the ratio of the power inside all the cladding tubes to the total power in the fiber geometry. For a fiber with 6 cladding tubes, the power ratio inside the tubes decreases by a factor of 3.8, when the gap increases from 0 to $10 \mu\text{m}$. For fibers with 8 and 10 cladding tubes, the power ratios inside the tubes only decrease by 22% and 21% when the gap increases from 0 to $10 \mu\text{m}$, respectively. This study shows that the gap has more impact on the power ratio inside the tubes for a fiber with 6 cladding tubes.

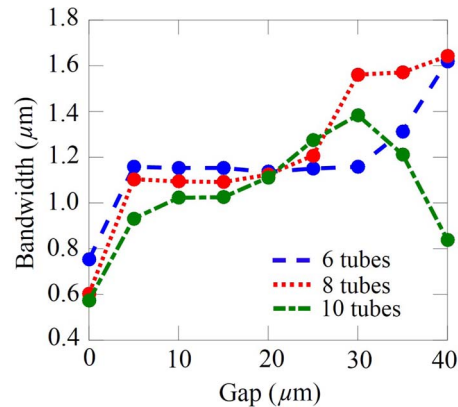


Fig. 9. Bandwidth as a function of the gap in fibers with six, eight, and ten cladding tubes. The tube wall thickness is $1.8 \mu\text{m}$.

We further study the normalized electric field intensity at $g = 0$ and $g = 10 \mu\text{m}$ in fibers with 6 and 8 cladding tubes. Fig. 8(a) shows one quarter of the fiber geometry with 6 cladding tubes. Fig. 8(c) shows the normalized electric field intensity in a fiber with 6 cladding tubes along x -axis at $y = 0$. We can see the mode is confined inside the core radius of $75 \mu\text{m}$ for both $g = 0$ and $g = 10 \mu\text{m}$. The thin gray vertical bar indicates the location of the glass tube at $x = 75 \mu\text{m}$ with a thickness of $1.8 \mu\text{m}$. The field between $x = 76.8 \mu\text{m}$ and $x = 203 \mu\text{m}$ is inside the cladding tube for the fiber with $g = 10 \mu\text{m}$ indicated by the red dashed curve, which shows exponential decay inside the cladding tubes. For the fiber with $g = 0$, the field between $x = 76.8 \mu\text{m}$ and $x = 223 \mu\text{m}$ is inside the cladding tube indicated by the blue solid curve, which shows noticeable field due to the weak coupling between the core mode and the tube modes. Note that the fiber with $g = 0$ has a cladding tube diameter of $146 \mu\text{m}$ that is close to the core diameter of $150 \mu\text{m}$. On the other hand, the fiber with $g = 10 \mu\text{m}$ has a cladding tube diameter of $126 \mu\text{m}$ that is much smaller than the core diameter. Hence, the gap effectively decreases the diameter of tube, which reduces the coupling between the core mode and the tube modes. The gap also induces an abrupt decrease in the power ratio inside the tubes, as shown in Fig. 7.

A quarter of the fiber geometry with 8 cladding tubes is shown in Fig. 8(b). In this case, the diameter of tube is much smaller than the diameter of the central air core. There is almost no coupling between the central air-core mode and the cladding-tube modes, and the electric field intensities decay exponentially along the x -axis in the cladding tubes for both $g = 0$ and $g = 10 \mu\text{m}$, as shown in Fig. 8(d). Hence, for a fiber with 8 or 10 cladding tubes, there is no sharp decrease in the power ratio inside the tubes when the gap first becomes non-zero, as shown in Fig. 7. The power ratio inside the tubes decreases almost linearly when the gap increases from 0 to $40 \mu\text{m}$. The optimal gap of $5 \mu\text{m}$ to $10 \mu\text{m}$ for the fiber with 8 or 10 cladding tubes is much smaller than the optimal gap of $30 \mu\text{m}$ for a fiber with 6 cladding tubes, which is needed to remove the weak coupling between the core mode and the tube modes. In Fig. 8, we show the light intensity with the electric field polarized in the x -direction. The other polarization yields similar results.

In nested negative curvature fibers, where another nested tube is inside each major lattice tube, a small gap should be used to minimize the loss [26]. A much larger gap should be used in standard negative curvature fibers with six cladding tubes, as shown in Fig. 1, because a weak coupling between the core mode and tube modes plays an important role in this case and must be minimized.

Fig. 9 shows a bandwidth comparison among fibers with 6, 8, and 10 cladding tubes. The blue dashed curve is the same as the blue dashed curve in Fig. 5(a). When the gap increases from 0 to $5 \mu\text{m}$, the bandwidth increases sharply due to the removal of the nodes from the connecting tubes. The bandwidths for fibers with 6 and 8 cladding tubes further increase as the gap

increases from 25 μm to 40 μm , with the tradeoff of increased leakage loss at the central wavelength. For a fiber with 10 tubes, the tube diameter is too small to confine the mode in the core when the gap is 40 μm , as shown in Fig. 6. The bandwidth for a fiber with 10 tubes also decreases accordingly when the gap is 40 μm , as shown in Fig. 9.

6. Conclusion

In this paper, we design tube structure in chalcogenide negative curvature fibers. Fibers with tube wall thicknesses of 0.7 μm , 1.8 μm , and 2.9 μm satisfy an antiresonance condition and have the minimum leakage loss at a wavelength of 5 μm . The gap can effectively decrease the transmission loss by a factor of 19 in the negative curvature fiber with 6 cladding tubes. We find that there is a range of the gaps, which correspond to a low leakage loss and a wide transmission bandwidth. Using a fiber with a tube wall thickness of 1.8 μm and a gap range between 5 μm and 40 μm , a low transmission loss of under 0.04 dB/m and a bandwidth of 1.1 μm can be achieved simultaneously in chalcogenide negative curvature fibers. It is found that a lower-order transmission band yields a wider bandwidth than the bandwidth from a higher-order transmission band. The optimal gap corresponding to the minimum loss in a fiber with 6 cladding tubes is 3 times as large as the optimal gap in fibers with 8 or 10 cladding tubes. A larger gap is required to remove the weak coupling between the core mode and tube modes in a fiber with 6 cladding tubes. In summary, a fiber design with low sensitivity to exact gaps allows low-loss and broadband chalcogenide fiber devices even with some uncertainties in the fiber drawing process.

Acknowledgment

We thank Dr. R. J. Weiblen for carrying out additional simulations to verify the results in this paper.

References

- [1] J. C. Knight, J. Broeng, T. A. Birks, and P. S. J. Russell, "Photonic band gap guidance in optical fibers," *Science*, vol. 282, no. 5393, pp. 1476–1478, Nov. 1998.
- [2] P. J. Roberts *et al.*, "Ultimate low loss of hollow-core photonic crystal fibres," *Opt. Exp.*, vol. 13, no. 1, pp. 236–244, Jan. 2005.
- [3] C. M. Smith *et al.*, "Low-loss hollow-core silica/air photonic bandgap fibre," *Nature*, vol. 424, no. 6949, pp. 657–659, Aug. 2003.
- [4] F. Poletti, M. N. Petrovich, and D. J. Richardson, "Hollow-core photonic bandgap fibers: Technology and applications," *Nanophotonics*, vol. 2, no. 5/6, pp. 315–340, Dec. 2013.
- [5] J. Hu and C. R. Menyuk, "Leakage loss and bandgap analysis in air-core photonic bandgap fiber for nonsilica glasses," *Opt. Exp.*, vol. 15, no. 2, pp. 339–349, Jan. 2007.
- [6] A. D. Pryamikov, A. S. Biriukov, A. F. Kosolapov, V. G. Plotnichenko, S. L. Semjonov, and E. M. Dianov, "Demonstration of a waveguide regime for a silica hollow-core microstructured optical fiber with a negative curvature of the core boundary in the spectral region $> 3.5 \mu\text{m}$," *Opt. Exp.*, vol. 19, no. 2, pp. 1441–1448, Jan. 2011.
- [7] F. Yu, W. J. Wadsworth, and J. C. Knight, "Low loss silica hollow core fibers for 3–4 μm spectral region," *Opt. Exp.*, vol. 20, no. 10, pp. 11153–11158, May 2012.
- [8] V. Setti, L. Vincetti, and A. Argyros, "Flexible tube lattice fibers for terahertz applications," *Opt. Exp.*, vol. 21, no. 3, pp. 3388–3399, Feb. 2013.
- [9] W. Belardi and J. C. Knight, "Hollow antiresonant fibers with reduced attenuation," *Opt. Lett.*, vol. 39, no. 7, pp. 1853–1856, Apr. 2014.
- [10] W. Ding and Y. Wang, "Analytic model for light guidance in single wall hollow core anti-resonant fibers," *Opt. Exp.*, vol. 22, no. 22, pp. 27242–27256, Nov. 2014.
- [11] A. Hartung *et al.*, "Double antiresonant hollow core fiber-guidance in the deep ultraviolet by modified tunneling leaky modes," *Opt. Exp.*, vol. 22, no. 16, pp. 19131–19140, Aug. 2014.
- [12] W. Belardi and J. C. Knight, "Effect of core boundary curvature on the confinement losses of hollow antiresonant fibers," *Opt. Exp.*, vol. 21, no. 19, pp. 21912–21917, Sep. 2013.
- [13] C. Wei, R. A. Kuis, F. Chenard, C. R. Menyuk, and J. Hu, "Higher-order mode suppression in chalcogenide negative curvature fibers," *Opt. Exp.*, vol. 23, no. 12, pp. 15824–15832, Jun. 2015.
- [14] C. Wei, C. R. Menyuk, and J. Hu, "Bending-induced mode non-degeneracy and coupling in chalcogenide negative curvature fibers," *Opt. Exp.*, vol. 24, no. 11, pp. 12228–12239, May 2016.
- [15] M. S. Habib, O. Bang, and M. Bache, "Low-loss hollow-core silica fibers with adjacent nested anti-resonant tubes," *Opt. Exp.*, vol. 23, no. 13, pp. 17394–17406, Jun. 2015.
- [16] P. Uebel *et al.*, "Broadband robustly single-mode hollow-core PCF by resonant filtering of higher-order modes," *Opt. Lett.*, vol. 41, no. 14, pp. 1961–1964, May 2016.

- [17] N. Edavalath, M. H. Frosz, J. Ménard, and P. S. Russell, "Fabrication and side-coupling characterization of hexagonal lattice single-ring hollow-core PCFs," presented at the Frontiers in Optics, Optical Society of America, San Jose, CA, USA, 2015, paper: FM3G.3.
- [18] A. D. Pryamikov, A. F. Kosolapov, V. G. Plotnichenko, and E. M. Dianov, "Transmission of CO₂ laser radiation through glass hollow core microstructured fibers," in *CO₂ Laser-Optimisation and Application*, D. C. Dumitras, ed. Rijeka, Croatia: InTech, 2012.
- [19] Y. Wang, F. Couny, P. J. Roberts, and F. Benabid, "Low loss broadband transmission in optimized core-shaped Kagome hollow core PCF," in *Proc. Conf. Lasers Electro-Opt./Quant. Electron. Laser Sci.*, San Jose, CA, USA, 2010, pp. 1–2.
- [20] Y. Wang, N. V. Wheeler, F. Couny, P. J. Roberts, and F. Benabid, "Low loss broadband transmission in hypocycloid-core Kagome hollow-core photonic crystal fiber," *Opt. Lett.*, vol. 36, no. 5, pp. 669–671, Mar. 2011.
- [21] A. F. Kosolapov *et al.*, "Demonstration of CO₂-laser power delivery through chalcogenide-glass fiber with negative-curvature hollow core," *Opt. Exp.*, vol. 19, no. 25, pp. 25723–25728, Dec. 2011.
- [22] M. A. Duguay, Y. Kokubun, T. L. Koch, and L. Pfeiffer, "Antiresonant reflecting optical waveguides in SiO₂-Si multi-layer structures," *Appl. Phys. Lett.*, vol. 49, no. 13, pp. 13–15, Jul. 1986.
- [23] N. M. Litchinitser, A. K. Abeeluck, C. Headley, and B. J. Eggleton, "Antiresonant reflecting photonic crystal optical waveguides," *Opt. Lett.*, vol. 27, no. 18, pp. 1592–1594, Sep. 2002.
- [24] V. S. Shiryayev *et al.*, "Development of technique for preparation of As₂S₃ glass preforms for hollow core microstructured optical fibers," *J. Optoelectron. Adv. M.*, vol. 16, no. 9/10, pp. 1020–1025, Sep./Oct. 2014.
- [25] V. S. Shiryayev, "Chalcogenide glass hollow-core microstructured optical fibers," *Front. Mater.*, vol. 2, no. 24, pp. 1–10, Mar. 2015.
- [26] F. Poletti, "Nested antiresonant nodeless hollow core fiber," *Opt. Exp.*, vol. 22, no. 20, pp. 23807–23828, Oct. 2014.
- [27] A. N. Kolyadin, A. F. Kosolapov, A. D. Pryamikov, A. S. Biriukov, V. G. Plotnichenko, and E. M. Dianov, "Light transmission in negative curvature hollow core fiber in extremely high material loss region," *Opt. Exp.*, vol. 21, no. 8, pp. 9514–9519, Apr. 2013.
- [28] W. Belardi and J. C. Knight, "Hollow antiresonant fibers with low bending loss," *Opt. Exp.*, vol. 22, no. 8, pp. 10091–10096, Apr. 2014.
- [29] A. Schliesser, N. Picqué, and T. W. Hänsch, "Mid-infrared frequency combs," *Nat. Photon.*, vol. 6, no. 7, pp. 440–449, Jun. 2012.
- [30] J. Hu and C. R. Menyuk, "Understanding leaky modes: Slab waveguide revisited," *Adv. Opt. Photon.*, vol. 1, no. 1, pp. 58–106, Jan. 2009.
- [31] Y. Yao, J. A. Hoffman, and C. F. Gmachl, "Mid-infrared quantum cascade lasers," *Nat. Photon.*, vol. 6, no. 7, pp. 432–439, Jun. 2012.
- [32] T. P. White *et al.*, "Multipole method for microstructured optical fibers. I. Formulation," *J. Opt. Soc. Amer. B, Opt. Phys.*, vol. 19, no. 10, pp. 2322–2330, Oct. 2002.
- [33] G. Ren, Z. Wang, S. Lou, and S. Jian, "Mode classification and degeneracy in photonic crystal fibers," *Opt. Exp.*, vol. 11, no. 11, pp. 1310–1321, Jun. 2003.
- [34] W. Xing, J. Bai, and Y. Li, "Mode classification and calculation in all-solid photonic bandgap fibers," *J. Lightw. Technol.*, vol. 30, no. 6, pp. 821–828, Mar. 2012.
- [35] M. Michieletto, J. K. Lyngsø, C. Jakobsen, J. Lægsgaard, O. Bang, and T. T. Alkeskjold, "Hollow-core fibres for high power pulse delivery," *Opt. Exp.*, vol. 24, no. 7, pp. 7103–7119, Mar. 2016.
- [36] K. Saitoh and M. Koshiba, "Leakage loss and group velocity dispersion in air-core photonic bandgap fibers," *Opt. Exp.*, vol. 11, no. 23, pp. 3100–3109, Nov. 2003.
- [37] J. Hu, C. R. Menyuk, L. B. Shaw, J. S. Sanghera, and I. D. Aggarwal, "Computational study of a 3–5 μm source that is created by using supercontinuum generation in As₂S₃ chalcogenide fibers with a pump at 2 μm," *Opt. Lett.*, vol. 35, no. 17, pp. 2907–2909, Sep. 2010.
- [38] V. G. Ta'eed *et al.*, "Ultrafast all-optical chalcogenide glass photonic circuits," *Opt. Exp.*, vol. 15, no. 15, pp. 9205–9221, Jul. 2007.
- [39] P. Klocek, *Handbook of Infrared Optical Materials*. New York, NY, USA: CRC Press, 1991.